Available online at www.sciencedirect.com
ScienceDirect
Radiation Physics and Chemistry 75 (2006) 2165–2173
Radiation Physics and Chemistry
www.elsevier.com/locate/radphyschem

Investigations on compton scattering: New directions

B.K. Chatterjee[a], L.A. LaJohn[b], S.C. Roy[a,*]

[a]Department of Physics, Bose Institute, 93/1 Acharya Prafulla Chandra Road, Kolkata 700009, India
[b]Department of Physics and Astronomy, University of Pittsburgh, Pittsburgh, PA 15260, USA

Received 30 July 2004; accepted 24 March 2006

Abstract

Although inelastic (Compton) scattering of a photon off a free electron was well understood about 80 years ago, inelastic scattering off bound electrons remains an incompletely understood process. The availability of synchrotron light sources has led a great enhancement in the precision of experimental measurements involving this process. As a result, approximations made in obtaining numerical predictions of physical observables are being reexamined by theorists. In this article, we present a comparison of experimental measurements to theoretical predictions to assess the need for future advances in both experiment and theory.

Keywords: Compton scattering; *S*-matrix; Impulse approximation; Incoherent scattering factor; Photons

1. Introduction

Compton scattering is the inelastic scattering of photons (X-rays and gamma rays) by the electrons bound to the atom. A schematic diagram of Compton scattering is presented in Fig. 1. An incident photon of energy $h\nu_i$ is scattered by the electron at an angle θ with an energy $h\nu_f$. The energy of the scattered photon is less than the incident photon energy. Classical electromagnetic theory cannot explain the observed inelastic component of the scattering of electromagnetic radiation from charged particles. Compton (1923) and Compton and Hubbard (1923) derived an expression for the energy of the scattered photon when deflected by an angle θ by a free, stationary electron. The description depends both on applications of relativistic kinematics and on a particle description of the photon. Under the assumption that the scattering electron is free and initially at rest, the scattered photon energy is

$$(h\nu_f)_{free} = \frac{h\nu_i}{1 + (h\nu_i/mc^2)(1 - \cos\theta)}. \quad (1)$$

Thus we see that in scattering from free and stationary electrons, the outgoing photon energy is uniquely defined by its scattering angle. However, in almost all practical cases of scattering, electrons are not free but bound to the target atom. In such scattering the following situation may arise: the electron is ejected leaving the atom in an ionized state or it is excited leaving the atom in an excited state. These two possible processes are distinguished by their names: the former one is known as Compton scattering while the latter one is known as Raman scattering. The one thing common in both cases is that the scattered photon has less energy than the incoming photon and hence both Raman and Compton scattering are inelastic scattering. In this present discussion we are concerned only with Compton scattering in which the final state consists of the scattered photon, the ejected electron and an ionized

*Corresponding author. Tel.: +91 33 2350 2402; fax: +91 33 2350 6790.
E-mail addresses: sup_roy@yahoo.com, scroy@bosemain.boseinst.ac.in (S.C. Roy).

0969-806X/$ - see front matter © 2006 Elsevier Ltd. All rights reserved.
doi:10.1016/j.radphyschem.2006.03.073

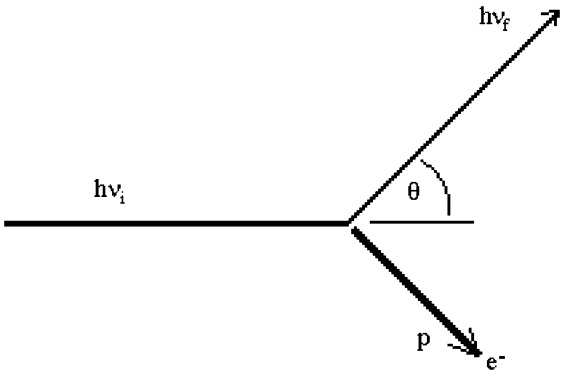

Fig. 1. Schematic representation of Compton scattering.

atom, which while returning to its ground state, may emit fluorescence photons or Auger electrons.

For a given incident photon energy and polarization, one can measure the energies, polarizations and angles of the scattered photon, the ejected electron, and subsequent transition radiation. However, here we will only discuss cases in which at best only the energy and direction of the scattered photon and the direction of the ejected electron are observed and the photons are unpolarized. So far, measurements up to only three such variables in the form of $(d^3\sigma/d\Omega_\gamma d(h\nu_f)\, d\Omega_e)$ have been measured. Here Ω_γ and Ω_e are the solid angle of the emitted photon and ejected electron, respectively. We will give some discussion of the measurements of only the scattered photon intensity at any given angle with or without observing the scattered photon energy. The corresponding quantity of interest in the former case is the cross section doubly differential in scattered photon energy and angle $[(d^2\sigma/d\Omega_\gamma\, d(h\nu_f))]$, while the corresponding quantity in the latter case is the singly differential cross section in angle $(d\sigma/d\Omega_\gamma)$. The doubly differential cross section can be measured or calculated shellwise, while the singly differential cross section is most often obtained for the whole atom.

The purpose of the present paper is not to present an overview of Compton scattering, but to discuss the new approaches and directions that emerged out of the recent high precision scattering experiments performed using synchrotrons (Jung et al., 1998; Young et al., 2001; Namito et al., 1995; Southworth et al., 2000) coupled with the precise theoretical predictions using *S*-matrix theory developed at the University of Pittsburgh. Excellent review articles on Compton scattering are available (Kane, 1992, Bergstrom and Pratt, 1997; Kane, 1997). To that purpose, we will briefly discuss the effect of binding and the present status of theoretical understanding of the subject in Sections 2 and 3, respectively. The experimental measurements done in recent years, particularly at X-ray energies (tens of keVs), will be discussed in Section 4. In Section 5 we present a comparison of experimental measurements and theoretical predictions of various atomic Compton physical observables, and then we assess the need for future work in our conclusion.

2. Effect of binding

The most noticeable effect of binding of electrons is in the energy distribution of outgoing photons. Instead of a monoenergetic Compton line expected for scattering from a free electron (Eq. (1)), there is a distribution of energies. A schematic illustration of the main effects of binding on the scattered photon energy is presented in Fig. 2. The free Compton line is represented in the figure by a delta function in energy. This peak is substantially broadened in energy reflecting the fact that the electrons are not at rest. Du Mond (1929, 1930, 1933) first explained that the broadening of the Compton line results from the momentum distribution of the bound electrons. In his model, now known as the impulse approximation (IA), bound electrons were replaced by free electrons with momentum distributions determined by the bound electron wave functions. The amount of broadening depends on the width of the momentum distribution of the scatterer, and this width increases as the electron is confined to smaller distances (tightly bound). For tightly bound electrons, the Compton peak is broader, while the peak is narrower when the scattering occurs from valance electrons. If the scattering occurred from free charges in motion, one would expect that the peak would be centred at the energy of the free Compton line. However, what was observed is that the centre of the peak moves slightly from the free

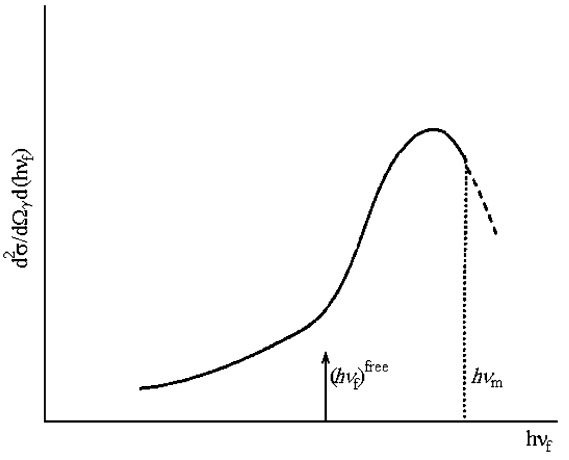

Fig. 2. Schematic illustration of the effect of binding on the Compton line is the broadening of the peak. $(h\nu_f)^{free}$ and $(h\nu_m)$ represent the free Compton energy and maximum energy from the kinematic limit, respectively.

electron value. This difference in energy from the free Compton line is known as the Compton defect. The direction and magnitude of the defect varies depending on the subshell of the electrons (Bloch and Mendelsohn, 1974). The kinematics of the process decides the maximum energy of the scattered photon. This energy is $h\nu_m = h\nu_i - B$, where B is the binding energy of the shell.

Another effect of binding may arise in a situation where the scattered photon energy is close to the difference between the initial state energy and the energy of another bound state. This region of the spectrum is called resonant Raman–Compton scattering. As the final state consists of a scattered photon, an ejected electron and the residual ion, this is a Compton scattering event. However, the intermediate state can be close to or on the energy shell, resulting in a resonant enhancement of the process. This resonant region was observed by Sparks (1974). Another interesting feature one can anticipate, when the scattered photon energy is very low, is the 'infrared divergence'. This infrared divergence is well known to be a consequence of quantum electrodynamics. Although theory unambiguously predicts the infrared divergence, there are no convincing experimental observations. While some measurements were reported of the observed infared divergence (Spitale and Bloom, 1977; Basavaraju et al., 1987; Briand et al., 1989), they were later challenged by others (Marchetti and Franck, 1989, 1990) or withdrawn, suggesting that the reported results were perhaps due to other phenomena such as bremsstrahlung following photoeffect. Manninen et al. (1990) later observed an infrared rise, but concluded that it was due entirely to photoelectron bremmsstrahlung in the target.

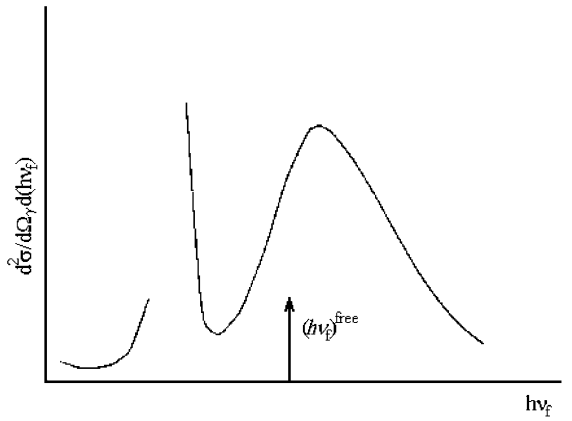

Fig. 3. Schematic illustration of all the expected features of Compton scattering. Figure shows the Compton peak followed by resonance region, infrared rise, which diverges as photon energy approaches zero.

The complete description of the general features of the energy distribution of the Compton cross section is presented in Fig. 3. If we start from the right, it contains a broadened peak region, followed with a resonance region, and an infrared rise as we move to lower photon energies and it diverges as the photon energy approaches zero. We will see in the next section which of the existing theoretical calculations can predict the entire range of the spectrum.

3. Theoretical schemes

The theory of compton scattering is, in general, based on the relativistic treatment of the interaction between the electromagnetic field and bound electrons. However, the non-relativistic interaction Hamiltonian is of the form:

$$H_{\text{int}} = \frac{e^2}{2mc^2}A^2 - \frac{e}{mc}p.A, \tag{2}$$

where p is the electron momentum and $\boldsymbol{A}$ is the vector potential of the electromagnetic field. The important concepts in constructing simpler approaches to scattering are to consider scattering from free charges, neglecting the binding of electrons to the atom. Except for the work of Gavrila (1972a, b), all non-relativistic treatments of Compton scattering by bound electrons that have been given so far are based on the A^2 approximation. Most commonly available theories of Compton scattering, except S-matrix calculation, and the work of Gavrila are based on scattering from free electrons.

3.1. Klein–Nishina formula

It is the simplest of all available methods to calculate the single differential Compton scattering cross sections. Using relativistic quantum theory to the scattering from a free electron at rest, Klein and Nishina (1929) first derived an expression of the cross section singly differential in scattered photon angle as given by

$$\frac{d\sigma}{d\Omega_\gamma} = \frac{r_0^2}{2}\left(\frac{(h\nu_f)^{\text{free}}}{h\nu_i}\right)^2\left(\frac{(h\nu_f)^{\text{free}}}{h\nu_i} + \frac{h\nu_i}{(h\nu_f)^{\text{free}}} - \sin^2\theta\right). \tag{3}$$

Since this expression is obtained on the assumption that electrons are free, it has a very limited applicability, although it is still very widely used.

3.2. Incoherent scattering factor approximation

This approximation is used to calculate the single differential cross section $(d\sigma/d\Omega_\gamma)$ for bound electron Compton scattering. The incoherent scattering factor (ISF) commonly symbolized by $S(x,Z)$ when multiplied

by the Klein–Nishina cross section gives an estimate of $(d\sigma/d\Omega_\gamma)$ modified due to the binding of electrons. Here $x = 2(h\nu_i/c)\sin(\theta/2)$ is the momentum transferred in the scattering and Z is the atomic number of the target element. ISF uses a closure approximation in its derivation, involving a sum over all inelastic procedures (including excitations). As a result, it calculates Compton scattering plus Raman scattering. Kinematic restrictions on allowed transitions (due to binding) are ignored in ISF. Details of the ISF calculation, and frequently used tables of scattering factors $S(x,Z)$ at different momentum transfers and atomic numbers are given by Hubbell et al. (1975). ISF is, in a sense, a measure of the number of electrons that contribute to the scattering as if they were free electrons. For high incident photon energies and momentum transfers, the value of the ISF tends to the number of electrons in the atom (Z) and at very low momentum transfer, it tends to zero. In general, ISF agrees reasonably well with experiments for relatively larger momentum transfers. ISF results in general agree reasonably well with experimental measurements except at very low momentum transfers. A simpler method of evaluating ISF when the form factor (F) for elastic scattering is known reasonably well using the relationship $Z = F + S$ has been indicated by Chatterjee et al. (2004) for limited cases. Test of the validity of this method in a wider context are warranted.

3.3. Impulse approximation

In the IA, scattering is treated as if it occurs from free electrons modified by the initial momentum distribution determined by the wave function of the scatterer. IA is the most widely used method for obtaining Compton scattering cross sections in the peak region of the spectrum. The doubly differential cross section for Compton scattering within the non-relativistic IA may be expressed as (Eisenberger and Platzmann, 1970)

$$\frac{d^2\sigma}{d\Omega_\gamma d(h\nu_f)} = \frac{r_0^2}{2}\left(1+\cos^2\theta\right)\frac{v_f}{Kv_i}J_{nl}(p_z), \tag{4}$$

where $J_{nl}(p_z) = \iint dp_x\, dp_y \rho(p)$ is called the Compton profile. Tables of Compton profiles for all subshells of all elements are given by Biggs et al. (1975). IA is widely used in calculating cross sections, because it is reasonably accurate, yet simple to use. However, because it is derived assuming scattering from free electrons, the non-relativistic IA exhibits neither the infrared divergence nor the resonant structure in the cross section as presented in Fig. 3.

By application of relativistic kinematics to a photon beam colliding with a beam of moving electrons, Ribberfors (1975a, b) derived the relativistic IA. Relativistic like nonrelativistic IA does not fully account for the infrared divergence or for the resonant structures, since it is also based on the notion that the electron that scatters the photon is free. In the peak region of the spectrum both relativistic and non-relativistic IA agree well with exact results for scattering off outer electrons, while relativistic IA is generally in better agreement than non-relativistic IA predictions for scattering from inner shell electrons.

3.4. S-matrix calculation

The S-matrix calculation that we will discuss is based on the treatment of inelastic scattering of a photon by electrons bound in an atom by QED theory. The non-relativistic version of this theory within the independent particle approximation (IPA) involves treating in first order the A^2 operator in H_{int} (see Eq. (2) also Fig. 4a) and in second-order operator $\boldsymbol{p}\cdot\boldsymbol{A}$ (see Fig. 4b and c). In the relativistic theory these correspond to the treatment of $\boldsymbol{\alpha}\cdot\boldsymbol{A}$. Higher orders of perturbation, involving the electromagnetic interaction are required if one were to account for the correlated motions of the electrons. Early attempts to obtain relativistic S-matrix amplitude had been made by Whittingham (1971,1981) and by Witttwer (1972). One may construct the corresponding S-matrix amplitude as was achieved by Suric et al. (1991) and Bergstrom et al. (1993). A numerical code to calculate the S-matrix amplitude and cross section resulted from these efforts and is available at the University of Pittsburgh.

The first diagram, Fig. 4(a), representing the non-relativistic A^2 interaction would correspond to the Compton peak region of the energy spectrum shown in Fig. 3. The broadening of the free Compton energy cross section comes through the square of the Fourier

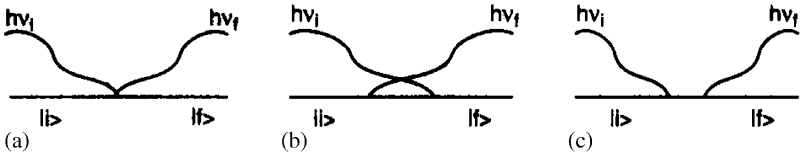

Fig. 4. Diagram representing the non-relativistic Compton scattering amplitudes: (a) is the seagull diagram of the A^2 interaction; (b) and (c) represent the second order contributions of the $\boldsymbol{p}\cdot\boldsymbol{A}$ interaction representing resonance and infrared divergence respectively (*Source*: Bergstrom and Pratt, 1997).

transform of the wavefunction of the electron that scatters the photon. The second diagram Fig. 4(b) becomes important when the scattered photon energy is close to the difference between the initial state energy and the energy of another bound state. The other bound state must be of lower energy as the photon is emitted first in this IPA single-electron transition diagram. In such cases, there are poles in the amplitude that enhance the scattering and represents the resonance region of the spectrum in Fig. 3. The third diagram Fig. 4(c) includes the region of infrared rise shown in Fig. 3. At low scattered photon energy, a relationship between the Compton scattering amplitude and the photoeffect amplitude exits. The Compton scattering amplitude in this limit is proportional to the photoeffect differential cross section and inversely proportional to the scattered photon energy. In the limit of zero scattered photon energy, the cross section diverges. In most cases, *S*-matrix theory can make accurate predictions over the entire spectrum unlike IA theory.

4. Experiment

The discovery of Compton scattering was made using an X-ray tube with an ionization chamber as the detector and a carbon foil as target. With the improvements of radiation sources and detectors, Compton scattering measurements were reinitiated from time to time and the basic understanding of the process was improved. Measurements of the singly differential cross section $(d\sigma/d\Omega_\gamma)$ i.e. the scattering cross section integrated over scattered photon energies, electron energies, and electron directions are the simplest and are the most extensive. Numerous measurements of the doubly differential scattering cross sections $(d^2\sigma/d\Omega_\gamma\, d\nu_f)$ have also been made. A few measurements of the triply differential cross sections $(d^3\sigma/d\Omega_\gamma\, d\nu_f\, d\Omega_e)$ integrated over electron directions have been reported (Bell et al., 1990, 1991; Kurp et al., 1996). Scattered photons detected in coincidence, for example, with characteristic *K* X-rays led to selective study of *K*-shell Compton scattering. A few measurements on *L*-shell scattering have also been reported. A survey on experimental studies on Compton and inelastic scattering measurements are available in the literature (Chakrabarty et al., 1991; Kane, 1992; Kane, 1997).

The availability of synchrotron sources with high resolution crystal monochromators coupled with high resolution detectors made possible precise experimental results with an uncertainty of 1–2% (Jung et al., 1998; Young et al., 2001; Southworth et al., 2000; Namito et al., 1995). All of these synchrotron measurements have been performed in order to obtain whole atom singly differential cross sections for a few elements at low photon energies (up to few tens of keVs). It has already been observed that experimental values of singly differential cross sections agree fairly well with ISF predictions at high photon energies and for large momentum transfers. Our interest was to compare cross sections obtained from only beams emitted from X-ray tubes to those obtained from synchrotron sources. Measurements using solid-state detectors have been considered in this report. We will describe how the improved accuracy of experimental data obtained by using synchrotron light sources has led to a reevaluation of the validity of many different theoretical methods for making predictions of the quantitative values obtained from such measurements.

5. Comparison of experiment with theories

Of course, no theoretical treatment of Compton scattering is completely accurate. Even the *S*-matrix calculation method developed at the University of Pittsburgh does not include nonlocal exchange and electron correlations effects, since it is based on a Dirac–Slater central potential. IA and ISF are known to neglect or incompletely treat the dynamic $\boldsymbol{p}\cdot\boldsymbol{A}$ term in the interaction Hamiltonian. Carney and Pratt (2000) estimated the magnitude of the various corrections associated with different theories (dynamic, non-local exchange, electron correlation and relativistic effects) and developed a general scheme to obtain "best" predictions. A prescription to obtain "best" predictions from any theoretical prediction, given by Carney and Pratt (2000), is to add the omitted corrections assuming that they are linearly independent perturbative corrections. This may be written as

$$\left(\frac{d\sigma}{d\Omega_\gamma}\right)_{\text{best}} = \left(\frac{d\sigma}{d\Omega_\gamma}\right)_{\text{theory}} \left(1 + \sum_j \delta_j\right). \tag{5}$$

Here $(d\sigma/d\Omega_\gamma)_{\text{theory}}$ represents any of the theoretical predictions (*S*-matrix, ISF, IA) and the summation is over the corrections δ_j relevant to the theory used. In both ISF and IA, there are corrections from the neglect of dynamic $\boldsymbol{p}\cdot\boldsymbol{A}$ term, other corrections to IA in A^2 This correction is known to be large at low momentum transfers. The Compton dynamic term is composed of both the contribution of the $\boldsymbol{p}\cdot\boldsymbol{A}$ term and the difference between the IA and exact evaluation of the A^2 term. A comparison of *S*-matrix results, ISF results and "best" predictions has been presented for neon at five photon energies and four scattering angles (Carney and Pratt, 2000). As a typical example, *S*-matrix and "best" results agree within about 10% for photon energies up to 5 keV, within about 2% for photon energies of about 10 KeV and within less than a percent for energies say above 20 keV for neon and at scattering angle of 90°.

Comparison of experimental results with ISF predicted and "best" results for neon has been made by Roy and Pratt (2004). Experimental Compton scattering cross sections have been derived from the measured Compton to Raleigh ratio (Jung et al., 1998) by using the "best" predicted Raleigh scattering cross sections (Carney and Pratt, 2000). We see that there is hardly any difference between ISF and "best" predicted values at higher photon energies. This is expected, as ISF is believed to be valid at higher photon energies. ISF is found to differ from "best" predicted values at lower photon energies: the difference is as much as 19% for 5.415 keV and 38% at 1.486 keV (see Fig. 5). This difference might be due to the neglect of dynamic $(\boldsymbol{p}\cdot\boldsymbol{A})$ scattering in ISF, which becomes important at lower photon energies. The ISF result of Hubbell et al. (1975) included excitation channels as well as ionization and therefore includes Raman scattering, while the "best" predictions presented here is only for Compton scattering. However, it has been found by Young et al. (2001) that the Raman contribution to total scattering is less than 1% for neon in the range 5–15 keV. Therefore, the large difference between ISF and "best" predictions at lower energies reflects the importance of dynamic corrections. However, use of perturbative corrections to obtain "best" predictions is questionable at lower energies. Under this situation, further measurements around 10 keV and lower are needed to confirm the adequacy of the theoretical treatment. But measurements of Compton scattering cross sections are challenging in this situation not only because that cross sections are smaller but also due to the fact that separation of the elastic and inelastic peaks will be difficult and may be beyond the capability of the present detector.

A comparison of experimental results obtained using conventional photon sources vis-a-vis synchrotron sources with ISF predicted values has been made by

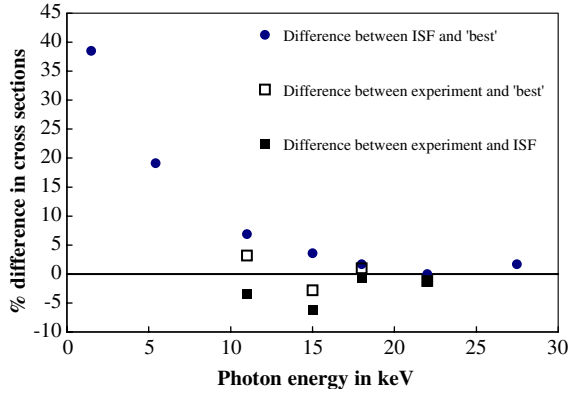

Fig. 5. Percent difference between ISF and "best", experiment (Jung et al., 1998) and ISF, and experiment (Jung et al., 1998) and "best" predicted values, for neon at 90° scattering angle (*Source*: Roy and Pratt, 2004).

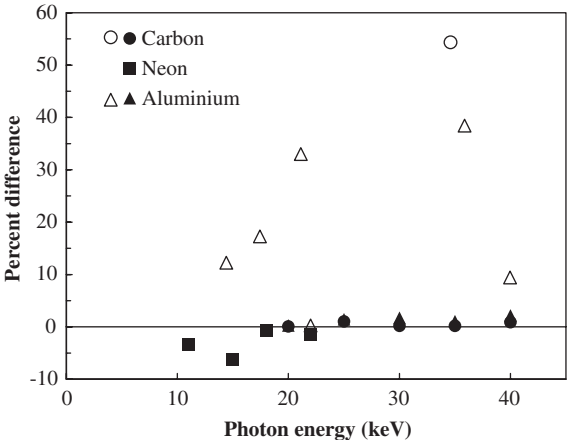

Fig. 6. Comparison of experimental Compton scattering cross sections (Garg et al., 1993; Rao et al., 1994; Namito et al., 1995; Jung et al., 1998) for carbon ($Z = 6$), neon ($Z = 10$) and aluminium ($Z = 13$), measured using conventional and synchrotron sources with ISF predicted values. Solid symbols represent measurements using synchrotron sources and hollow symbols represent measurements with conventional sources (*Source*: Roy and Pratt, 2004).

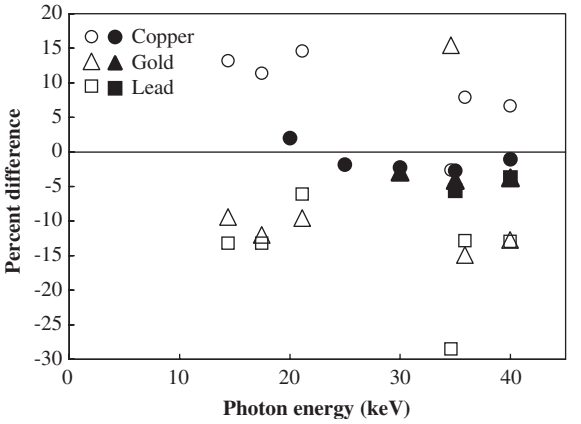

Fig. 7. Comparison of experimental Compton scattering cross sections (Garg et al., 1993; Namito et al., 1995 and Rao et al., 1994, 1996) for Copper ($Z = 29$), gold ($Z = 79$) and lead ($Z = 82$), measured using conventional and synchrotron sources, with ISF predicted values. Solid symbols represent measurements using synchrotron sources and hollow symbols represent measurements with conventional sources (*Source*: Roy and Pratt, 2004).

Roy and Pratt (2004). Figs. 6 and 7 exhibit a sharp contrast between the two types of measurements. Measurements using conventional sources are scattered, differing in magnitude from ISF by 5% to more than 50% (much above the stated uncertainties of 10%), while all measurements using synchrotron sources fall within a narrow band of few percent differences (mostly within the stated experimental uncertainties). Another

noticeable feature is that measured cross sections (using conventional sources) for lighter elements (up to copper here) are, in general, found to be larger than the ISF values while those for relatively heavier elements are less than the ISF. It may be mentioned that use of synchrotron sources, particularly in coincidence experiments, has been is seriously questioned due to the high random coincidence rate due to the pulsed nature of the beam (Laukkanen et al., 1996).

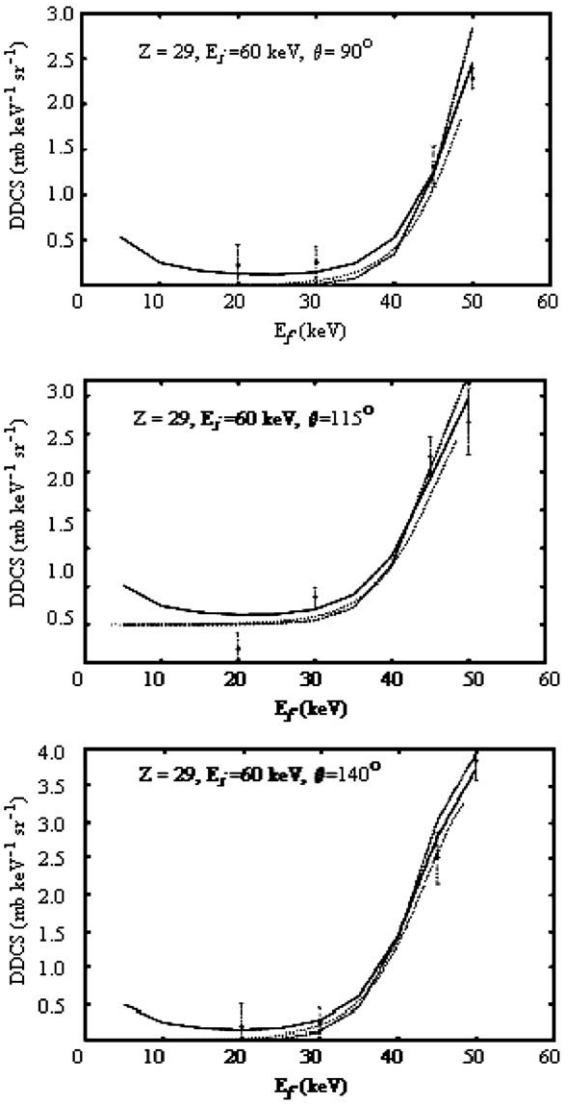

Fig. 8. Double differential cross sections (DDCS) for Compton scattering of 60 keV photons off Cu atoms resulting in the ejection of a *K*-shell electron at three different scattering angles (90°, 115° 140°). Solid line; *S*-matrix calculation using a Dirac Slater potential: dark dashed line; relativistic impulse approximation of Ribberfors (1975b): light dashed lines; nonrelativistic impulse approximation: crosses with error bars; measured double differential cross sections of Laukkanen et al. (1996).

Doubly differential cross sections for Compton scattering of 60 keV photons off *K*-shell electrons of copper atoms at three different scattering angles (90°, 115° and 140°) have been recently calculated at the University of Pittsburgh using the *S*-matrix code. Results have been compared with the non-relativistic and relativistic IAs and with the experimental results of Laukkanen et al. (1996) in Fig. 8. As expected, relativistic and non-relativistic IA results differ from *S*-matrix results more in the region of the low energy regime. It is clear from Fig. 8 that *S*-matrix results, in general, agree well with experimental values for all angles of scattering and for the entire range of the energy spectrum. Further measurements and theoretical calculations for different energies, angles and elements are needed to understand the general features of validity of theoretical calculations.

6. Conclusion

Recent high precision scattering experiments and the availability of precise theoretical values opened up new directions for future theoretical and experimental work on Compton scattering. There exists a scope to improve the understanding of Compton scattering by comparing cross sections predicted from the most advanced theoretical calculations with precise experimental results One of the areas requiring attention is low energy, inner shell scattering—the region where available theories are inadequate. Calculations and measurements for both single and double differential cross sections for total atom scattering and for scattering from electrons of different shells are needed. In order to understand the importance of dynamic aspects of scattering, which are not included in the simpler theoretical approaches, systematic investigations using the *S*-matrix code for a wide range of targets and photon energies are needed. It is expected that this will enable us to clarify the more detailed and intricate aspects of inelastic scattering, such as the infrared divergence and the resonance structures. ISF and "best" predicted results agree well at higher photon energies, but they were found to differ at energies below about 10 keV. At these energies it is known that ISF is not good due to the neglect of dynamic scattering term while the perturbative method used to obtain "best" predictions at lower energies may not be completely adequate, both because the various perturbations become large and because they are not necessarily independent.

Acknowledgements

The authors would like to thank Professor R.H. Pratt of the University of Pittsburgh, Pittsburgh for valuable

discussions. The manuscript was prepared under the auspices of Indo-US cooperative project "Investigations on theoretical aspects of Compton scattering" supported jointly by the Department of Science and Technology, Govt. of India and National Science Foundation of USA.

References

Basavaraju, G., Kane, P.P., George, S.M., 1987. A study of low energy photons resulting from Compton scattering of 279.2 keV gamma rays by *K*-shell electrons. Nucl. Instrum. Methods A 255, 86–89.

Bell, F., Rollason, A.J., Schneider, J.R., Drube, W., 1990. Determination of electron momentum densities by (gamma, *e* gamma) experiment. Phys. Rev. B. 41, 4887–4890.

Bell, F., Tschentscher, Th., Schneider, J.R., Rollason, A.J., 1991. The triple differential cross section for deep inelastic photon scattering. J. Phys. B 24, L533–L538.

Bergstrom, P.M., Suric, T., Pisk, K., Pratt, R.H., 1993. Compton scattering of photons from bound electrons:full relativistic independent particle approximation calculations. Phys. Rev. A 48, 1134–1162.

Bergstrom, P.M., Pratt, R.H., 1997. An overview of the theories used in Compton scattering calculations. Radiat. Phys. Chem. 50, 3–29.

Biggs, F., Mendelsohn, L.B., Mann, J.B., 1975. Hartree–Fock Compton profiles for the elements. At. Data Nucl. Data Tables 16, 201–309.

Bloch, B.J., Mendelsohn, L.B., 1974. Atomic *L*-shell Compton profiles and incoherent scattering factors: theory. Phys. Rev. A 9, 129–155.

Briand, J., Simionvici, A., Chevallier, P., Indelicato, P., 1989. Infrared divergence of the resonant Raman–Compton scattering. Phys. Rev. Lett. 62, 2092–2095.

Carney, J.P.J., Pratt, R.H., 2000. Constructing adequate predictions for photon-atom scattering: a composite approach. Phys. Rev. A. 62, 012705.

Chakrabarty, K., Roy, S.C., Sengupta, S.K., Pratt, R.H., 1991. Survey of Compton scattering experiments. Trans. Bose Res. Inst. 54, 1–29.

Chatterjee, B., Roy, S.C., Pratt, R.H., 2004. An alternative method to calculate inelastic scattering cross sections of photons. Radiat. Phys. Chem. 71, 679–680.

Compton, A.H., 1923. A quantum theory of the scattering of X-rays by light elements. Phys. Rev. 21, 483–502.

Compton, A.H., Hubbard, J.C., 1923. The recoil of electrons from scattered X-rays. Phys. Rev. 23, 439–449.

Du Mond, J.W.M., 1929. Compton modified line structure and its relation to the electron theory of solid bodies. Phys. Rev. 33, 643–658.

Du Mond, J.W.M., 1930. Breadth of Compton modified line. Phys. Rev. 36, 146–147.

Du Mond, J.W.M., 1933. The linear momenta of electrons in atoms and is solid bodies as revealed by X-ray scattering. Rev. Mod. Phys. 5, 1–33.

Eisenberger, P., Platzmann, P.M., 1970. Compton scattering of X-rays from bound electrons. Phys. Rev. A 2, 415–423.

Garg, M.L., Garg, R.R., Hennrich, F., Heimerman, D., 1993. Elastic and inelastic scattering of photons in the X-ray region. Nucl. Instrum. Methods B 73, 109–114.

Gavrila, M., 1972a. Compton scattering of photons by bound *K*-shell electrons—I. Non-relativistic theory with retardation. Phys. Rev. A 6, 1348–1359.

Gavrila, M., 1972b. Compton scattering of photons by bound *K*-shell electrons—II. Non-relativistic dipole approximation. Phys. Rev. A 6, 1360–1367.

Hubbell, J.H., Veigele, W.J., Briggs, E.A., Brown, R.T., Cromer, D.T., Howerton, R.J., 1975. Atomic form factors, incoherent scattering functions and photon cross sections. J. Phys. Chem. Ref. Data 4, 471–538.

Jung, M., Dunford, R.W., Gemmell, D.S., Kanter, E.P., LeBrun, T.W., Southworth, S.H., Young, L., Carney, J.P.J., Pratt, R.H., Bergstrom, P.M., 1998. Manifestation of non-local exchange, correlation, and dynamic effects in X-ray scattering. Phys. Rev. Lett. 81, 1596–1599.

Kane, P.P., 1992. Inelastic scattering of X-rays and gamma rays by inner shell electrons. Phys. Rep. 218, 67–139.

Kane, P.P., 1997. Experimental studies of inelastic X-ray and gamma ray scattering. Radiat. Phys. Chem. 50, 31–62.

Klein, O., Nishina, Y., 1929. Über die streuung von strahlung durch freie elektronen nach neuen relativistichen quantendynamik von Dirac. Z. Physik. 52, 853.

Kurp, F.F., Tschentscher, Th., Schulte-Schrepping, H., Schneider, J.R., Bell, F., 1996. 3D-electron momentum density of graphite. Europhys. Lett. 35, 61–66.

Laukkanen, J., Hämäläinen, K., Manninen, S., 1996. The absolute double-differential Compton scattering cross sections of Cu 1s electrons. J. Phys.: Condens. Matter 8, 2153–2162.

Manninen, S., Hämäläinen, K., Graeffe, J., 1990. Inelastic photon scattering from *K*-shell electrons of Cu and Zr. Phys. Rev. B 41, 1224–1226.

Marchetti, V., Franck, C., 1989. Inelastic X-ray scattering at intermediate momentum transfer: fluorescence spectrum and search for infrared divergence in scattered X-ray spectra. Phys. Rev. A 39, 647–657.

Marchetti, V., Franck, C., 1990. Comment on Infrared divergence of the resonant Raman–Compton scattering. Phys. Rev. Lett. 65, 268.

Namito, Y., Ban, S., Hirayama, H., Nariyama, N., Nakashima, H., Nakane, Y., Sakamoto, Y., Sasamoto, N., Asano, Y., Tanaka, S., 1995. Compton scattering of 20–40 keV photons. Phys. Rev. A 51, 3036–3043.

Rao, D.V., Cesareo, R., Gigante, G.E., 1994. Coherent and incoherent scattering of 14.93, 17.44, and 21.2 keV photons from Al, Cu, Sr, Cd, Ce, Pr, Sm, Pt, Au and Pb. Phys. Scr. 50, 314–320.

Rao, D.V., Cesareo, R., Gigante, G.E., 1996. Coherent and incoherent scattering of low energy X-rat photons in the atomic region $13 \leqslant Z \leqslant 82$. Can. J. Phys. 74, 10–16.

Ribberfors, R., 1975a. Relationship of the relativistic Compton cross section to the momentum distribution of bound electron states. Phys. Rev. B 12, 2067–2074.

Ribberfors, R., 1975b. Relationship of the relativistic Compton cross section to the momentum distribution of bound

electron states—II. Effects of anistropy and polarization. Phys. Rev. B 12, 3136–3141.

Roy, S.C., Pratt, R.H., 2004. Need for further inelastic scattering mesurements at X-ray energies. Radiat. Phys. Chem. 69, 193–197.

Sparks Jr., C.J., 1974. Inelastic resonance emission of X-rays: anomalous scattering associated with anomalous dispersion. Phys. Rev. Lett. 33, 262–265.

Spitale, G.C., Bloom, S.D., 1977. Incoherent scattering of gamma rays by *K*-shell electrons. Phys. Rev. A 16, 221–230.

Southworth, S.H., Young, L., Kanter, E.P., LeBrun, T.W., 2000. Photoionization and Photodetachment in Advanced Series in Physical Chemistry, No. 10B. Ng., C.Y. Ed., World Scientific, Singapore, pp. 1289–1334.

Suric, T., Pisk, K., Logan, B., Pratt, R.H., 1991. Compton scattering of photons by inner shell electrons. Phys. Rev. Lett. 67, 189–192.

Whittingham, I.B., 1971. Incoherent scattering of gamma rays in heavy atoms. J. Phys. A. 4, 21–37.

Whittingham, I.B., 1981. Compton Scattering of 279.1 and 661.6 keV photons by K-shell electrons. Aust. J. Phys. 34, 163–172.

Wittwer, L.A., 1972. K shell Compton scattering on tin and gold at 145 keV and gold at 302 keV. Ph.D. dissertation. University of California, Davis, California.

Young, L., Dunford, R.W., Kanter, E.P., Krassig, B., Southworth, S.H., Bonham, R.A., Lykos, P., Morong, C., Timm, A., Carney, J.P.J., Pratt, R.H., 2001. Corrections to the usual X-ray scattering factors in rare gases: experiment and theory. Phys. Rev. A 63, 052718.